Observations of surf beat propagation and energetics

Stephen M. Henderson[1], Steve Elgar[2], A.J.Bowen[1]

abstract

Near-bottom pressure and velocity, measured along a cross-shore transect extending from the shore to about 8-m water depth on a barred beach, are used to study the cross-shore propagation of surf beat and the associated cross-shore flux of surf beat energy. The dominant Empirical Orthogonal Functions (EOF's) of pressure fluctuations measured in less than 5 m depth at relatively low beat frequencies (0.005–0.025 Hz) had well developed nodes and antinodes, with $\pm\pi$ phase jumps at the nodes, suggestive of standing wave motions. The dominant EOF's of relatively high frequency surf beat (0.03–0.05 Hz) showed some nodal structure, but their phase increased approximately linearly with distance from the shore indicating net shoreward propagation. EOF's of combined pressure and cross-shore velocity fluctuations at beat frequencies showed a similar mixture of standing and progressive waves. Furthermore, phases between pressure and velocity components were close to $\pm\pi/2$ at relatively low beat frequencies (<0.25 Hz), as predicted by standing waves theories, but at higher beat frequencies (0.3–0.05 Hz) phases usually had magnitudes less than $\pi/2$, but significantly greater than zero, suggestive of mixed standing and shoreward progressive waves. Shoreward propagating surf beat carried a shoreward energy flux. During a storm, this shoreward flux was about half the flux that could have been carried if all surf beat propagated directly shorewards. The energy carried shoreward by propagating surf beat was lost either at the shoreface (for moderate waves) or on the offshore side of the bar (during a storm). On one occasion surf beat carried energy seawards outside the surf zone and shorewards inside the surf zone, consistent with theoretical models that predict surf beat forcing at the outer edge of the surf zone.

[1]Department of Oceanography, Dalhousie University, Halifax, Nova Scotia, B3H 4J1, Canada.
[2]AOPE, Woods Hole Oceanographic Institution, Woods Hole, MA 02534, USA.

1 Introduction

Gravity wave energy inside the surf zone sometimes is dominated by low frequency (0.005–0.05 Hz) waves known as surf beat. Unlike higher frequency incident waves, which are dissipated by breaking before they reach the shore, surf beat can be reflected strongly from the shore to form a cross-shore standing pattern. Holman (1981), Holland *et al.* (1995), and others presented field evidence for the existence of cross-shore standing waves at beat frequencies in water depths less than 4 m. However, Elgar *et al.* (1994) and Herbers *et al.* (1995) presented field evidence of significant net cross-shore surf beat propagation in 13-m water depth. Here, field observations of surf beat propagation in less than 7-m water depth are presented.

Propagating shallow water waves carry an energy flux that usually is directed away from regions of forcing and towards regions of dissipation. Thus, surf beat propagation is linked closely with surf beat forcing and dissipation.

The field site and instrumentation are described in section 2. In section 3 it is shown that spatially-coherent surf beat was partly cross-shore standing and partly cross-shore (usually shoreward) progressive. Estimates of the cross-shore energy flux carried by progressive surf beat are presented in section 4. Results are summarised in section 5.

2 Field site and instrumentation

Data were collected on an ocean beach near Duck, North Carolina, during the Duck94 experiment at the U.S. Army Field Research Facility (Gallagher *et al.*, 1998; Elgar *et al.*, 1997). Near-bottom water pressure and horizontal velocity were measured (at 2 Hz) at 15 locations along a cross-shore transect extending from the shore to about 8-m water depth (fig.1). Seabed elevations were determined with surveys from an amphibious vehicle (Lee and Birkemeier, 1993) and sonar altimeters (Gallagher *et al.*, 1996) co-located with the pressure and current sensors.

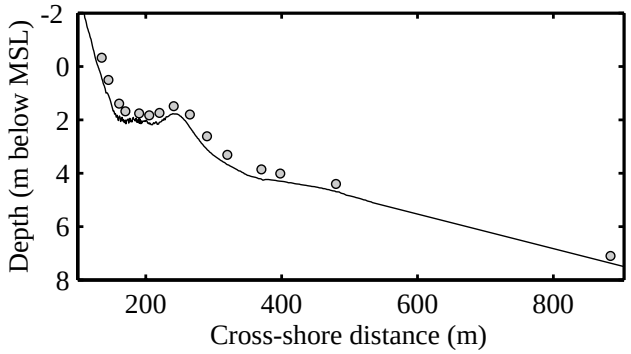

Figure 1: Beach profile measured on Sept. 20th (solid curve) and the location of co-located pressure gauges and current meters (circles). The zero of the x-axis is arbitrary.

3 Cross-shore structure of surf beat

3.1 Methods

At each instrument location, 3-hr time series of bottom pressure were broken into ninety 50% overlapping segments, with

$$p_{j,k}(t) = j\text{'th time series of bottom pressure at location } k.$$

Each time series segment was Hanning windowed and Fourier transformed. Let

$$dp_{j,k}(\sigma) = \text{Fourier component of windowed } p_{j,k} \text{ at frequency } \sigma,$$

$$\mathbf{dp}_j(\sigma) = \begin{pmatrix} dp_{j,1}(\sigma) \\ dp_{j,2}(\sigma) \\ \vdots \\ dp_{j,14}(\sigma) \end{pmatrix},$$

so that the vector $\mathbf{dp}_j(\sigma)$ represents the cross-shore structure of pressure fluctuations at frequency σ. Pressure fluctuations measured at the most offshore location (7.5 m depth, fig.1) were not included in $\mathbf{dp}_j(\sigma)$.

A cross-spectral matrix M_{pp} was estimated at every frequency σ,

$$M_{pp}(\sigma) = \overline{\mathbf{dp}_j(\sigma)\,\mathbf{dp}_j(\sigma)'},$$

where the overbar denotes an average over all realizations (i.e. all values of j), and $'$ denotes a conjugate transpose. At each frequency, the eigenvectors of $M_{pp}(\sigma)$ are the frequency-domain Empirical Orthogonal Functions (EOF's), or principal components, of the pressure fluctuations. There are as many EOF's as there are elements of $\mathbf{dp}_j(\sigma)$, but here only the dominant EOF is considered (i.e. the eigenvector of $M_{pp}(\sigma)$ associated with the largest eigenvalue). The dominant EOF is the single cross-shore structure that best fits the observed cross-shore structure of pressure fluctuations at frequency σ. In the cases presented the dominant EOF accounted for between 45% and 70% of the variance summed over all instruments.

If $\mathbf{x}(\sigma)$ is a dominant EOF, then so is $\alpha\,\mathbf{x}(\sigma)$ for any constant α. The EOF's are normalised so that the component representing the pressure fluctuation closest to the shore equals 1 m.

The combined pressure *and* cross-shore velocity EOF's also were estimated as the dominant eigenvectors of the cross-spectral matrix

$$M_{cc}(\sigma) = \overline{\mathbf{dc}_j(\sigma)\,\mathbf{dc}_j(\sigma)'},$$

where

$$\mathbf{dc}_j(\sigma) = \begin{pmatrix} \sqrt{g}\, dp_{j,1}(\sigma) \\ \sqrt{g}\, dp_{j,2}(\sigma) \\ \vdots \\ \sqrt{g}\, dp_{j,14}(\sigma) \\ \sqrt{h}\, du_{j,1}(\sigma) \\ \sqrt{h}\, du_{j,2}(\sigma) \\ \vdots \\ \sqrt{h}\, du_{j,14}(\sigma) \end{pmatrix},$$

$du_{j,k}(\sigma)$ =Fourier component of windowed $u_{j,k}$ at frequency σ,
$u_{j,k}(t)$ =j'th time series of shoreward water velocity at frame k,
g =gravitational acceleration,
h =water depth.

At every frequency a dominant EOF of was estimated from M_{cc}. This single dominant EOF represented the cross-shore structure of both pressure and velocity.

Note the energy-based weighting of dp and du (for shallow water waves $var[\sqrt{g}\, dp] =$ potential energy density at frequency σ and $var[\sqrt{h}\, du] =$ kinetic energy density at frequency σ).

Finally, the pressure components of the dominant EOF of M_{cc} were divided by $\sqrt{g}$ and the velocity components were divided by $\sqrt{h}$ to convert back to units of pressure (m) and velocity (ms^{-1}).

3.2 Results and discussion

Figure 2a–c shows the dominant EOF's of low frequency (0.022 Hz) pressure fluctuations for two different 3 hr pressure time series. Both EOF's have clear amplitude maxima (at the shore and $x \approx 230$ m) and minima (at $x \approx 160$ and $x \approx 300$ m), with a phase jump of $\pm\pi$ at each minimum, consistent with the presence of a cross-shore standing wave. Monotonic changes of phase with distance from the shore that indicate the presence of a cross-shore progressive wave were not observed.

The EOF's shown in fig.2a–c are typical of those observed at frequencies less than about 0.025 Hz. However at surf beat frequencies above about 0.030 Hz, the EOF's had a different cross-shore structure, as shown in fig. 2d–f ($\sigma = 0.044$ Hz). Although the higher-frequency EOF had some nodal structure (fig.2e), the phase jumps obvious in the low frequency case have been replaced by a monotonic increase in phase with distance from the shore (fig.2f), indicating the presence of some shoreward-progressive surf beat.

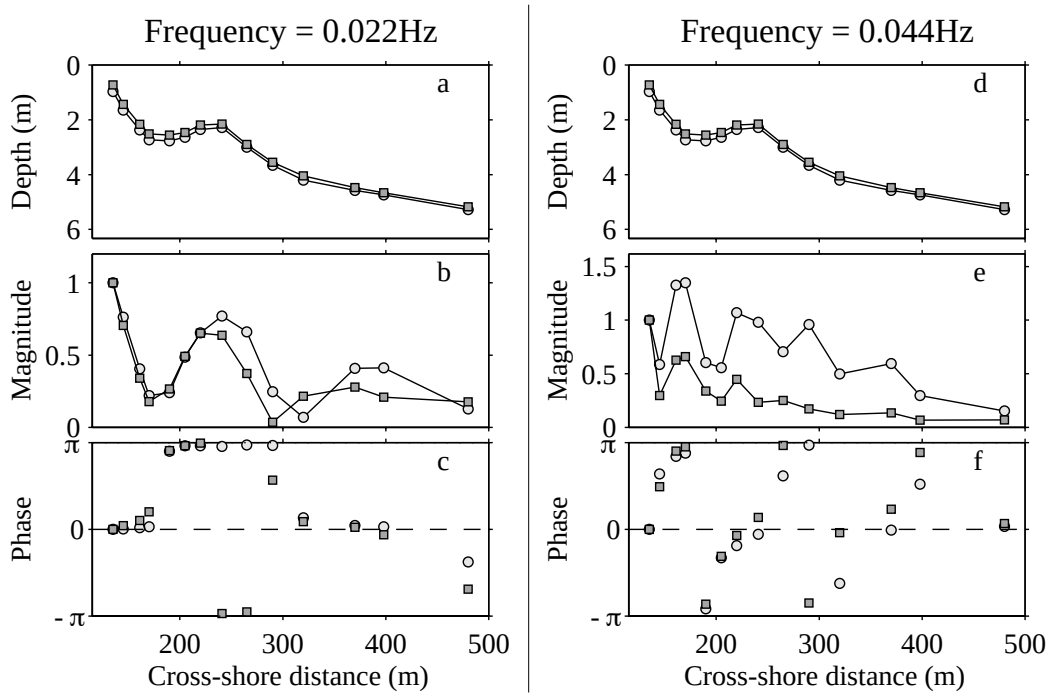

Figure 2: Water depth (a,d), and the amplitude in m (b,e) and phase (c,f) of dominant EOF's of pressure *versus* cross-shore distance (relative to same datum as fig.1). Left panels: frequency = 0.022 Hz. Right panels: frequency = 0.044 Hz. Squares: September 28th, significant wave height 0.4 m. Circles: September 22nd, significant wave height 2.7 m.

Figure 3a–c shows a dominant EOF of combined pressure and velocity fluctuations at $\sigma = 0.022$ Hz. Note that in fig.3b,c a single 28-element EOF, with 14 pressure components and 14 velocity components, is plotted as two curves, with one curve representing the cross-shore structure of pressure EOF components and the other representing the cross-shore structure of velocity EOF components. Also note that, although the absolute magnitude of the EOF is arbitrary, the relative magnitudes of the pressure and velocity components are not arbitrary. For example, if the EOF plotted in fig.3a–c had generated a pressure fluctuation of 1 m at the most onshore instrument location, the associated co-located velocity fluctuation would have been about 2 ms^{-1} (fig.3b).

The pressure component of the dominant EOF of combined pressure and velocity fluctuations (circles, fig.3b,c) is similar to the EOF of pressure fluctuations alone (circles, fig.2b,c). Contributions to both pressure and velocity fluctuations show nodes, antinodes, and $\pm\pi$ phase jumps. Offshore of $x \approx 200$ m the nodes of pressure fluctuations coincided with the antinodes of velocity fluctuations, and *vice-versa*. Onshore of $x \approx 390$ m pressures were about $\pm\pi/2$ out of phase with co-located velocities. All of of these features are predicted by cross-shore standing wave theories.

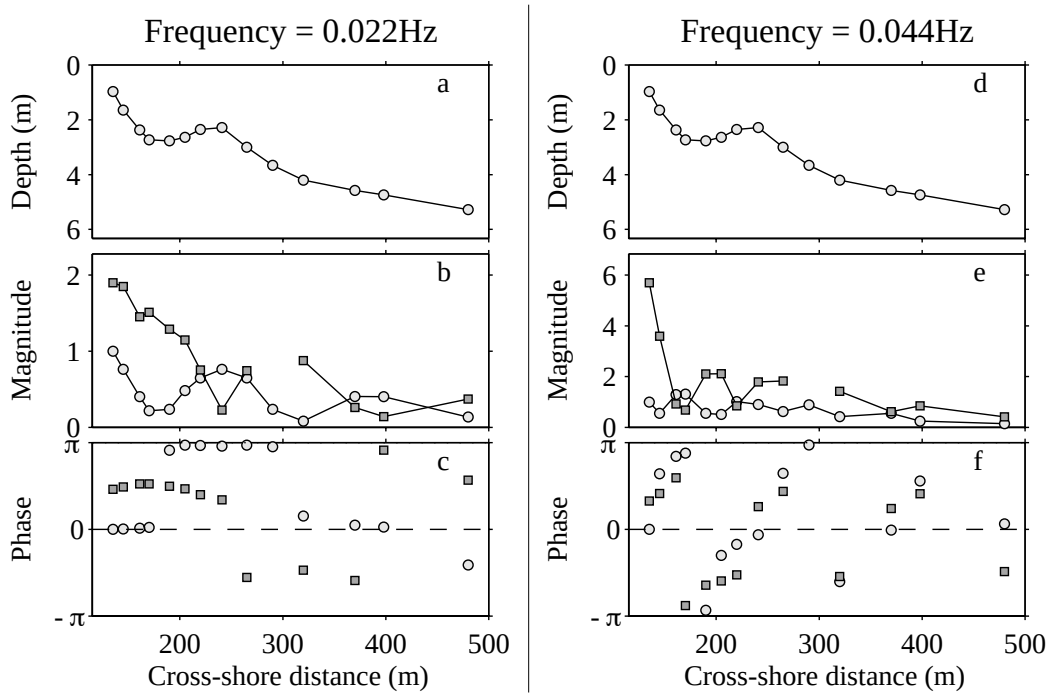

Figure 3: Water depth (a,d), and the amplitude (b,e) and phase (c,f) of the dominant EOF of combined water pressure and velocity on September 22nd *versus* cross-shore distance (relative to same datum as fig.1). Left panels: frequency = 0.022 Hz. Right panels: frequency = 0.044 Hz. Circles: pressure (m). Squares: cross-shore velocity (ms^{-1}).

The dominant EOF of combined water pressure and velocity fluctuations at 0.044 Hz displays a mixture of progressive and standing wave behaviours (fig.3d–f). Some nodal structure is present, but there is a monotonic increase in phase with distance from the shore, indicating net shoreward propagation. With the exception of the most offshore location, the magnitude of the phase between pressure and velocity was between the $\pm\pi/2$ phase of standing waves and the zero phase of shoreward progressive waves.

4 Surf beat energy flux

4.1 Methods

The energy flux q_{prog} of an undamped shoreward-propagating linear shallow water wave is

$$q_{prog} = E\,Cg,$$

where the energy density E in the frequency band between ω_1 and ω_2 is estimated as (Lippmann *et al.* (1999) discuss the accuracy of this approximation in the presence of

standing waves)

$$E = g \int_{\omega_1}^{\omega_2} \Phi_{\eta,\eta}(\omega)\, d\omega.$$

where $\Phi_{\eta,\eta}(\omega)$ is the power spectral density of the sea-surface elevation η at frequency ω. The group velocity $Cg = \sqrt{gh}$ in shallow water.

The energy flux q of directionally-spread linear shallow water waves with frequencies between ω_1 and ω_2 is

$$q = h \int_{\omega_1}^{\omega_2} \Re\{\Phi_{p,u}(\omega)\}\, d\omega$$

where $\Re\{\Phi_{p,u}(\omega)\}$ is the density of the co-spectrum between p and u at frequency ω.

Measured water depths and time series of p and u were used to estimate q_{prog} and q.

The nondimensional parameter

$$\rho = \frac{q}{q_{prog}},$$

indicates the cross-shore progressiveness of waves with frequencies between ω_1 and ω_2. If these waves propagate directly shoreward $\rho = 1$, if they propagate directly seaward $\rho = -1$, and if they are cross-shore standing $\rho = 0$.

The methods outlined in this section neglect the vertical structure associated with rollers and with waves that are not in shallow water. Consequently, the estimates of swell energy density and flux that are presented in the next section are not accurate and provide only a qualitative picture of swell energy and breaking. In contrast, estimates of surf beat energy densities and fluxes are probably not effected greatly by vertical structure.

4.2 Results and discussion

The estimated shoreward energy flux carried by moderately energetic swell (Sept. 16th, $Hs = 0.8$ m) decreased from about $2\ \mathrm{m^4 s^{-3}}$ at $x \approx 300$ m to about $0.7\ \mathrm{m^4 s^{-3}}$ at $x \approx 200$ m (fig. 4d). Presumably, the decrease of energy flux ($1.3\ \mathrm{m^4 s^{-3}}$) was caused by wave-breaking dissipation. For swell, the progressiveness parameter ρ was close to 1, but dropped slightly below 1 close to the shore (fig. 4f), indicating that swell was weakly reflected (consistent with Elgar *et al.* (1997)).

Onshore of $x \approx 200$ m surf beat carried energy shorewards ($q > 0$), whereas offshore of $x \approx 300$ m surf beat carried energy seawards ($q < 0$) (fig. 4e). Low frequency (high frequency) surf beat must have been generated at a net rate of about $0.02\ \mathrm{m^4 s^{-3}}$ ($0.03\ \mathrm{m^4 s^{-3}}$) between $x = 200$ and $x = 300$ m to replace the net flux of surf beat energy out of this region. In this region of surf beat forcing the swell energy flux decreased markedly due to breaking. Symonds *et al.* (1982) suggested that surf beat is forced at the outer edge of the surf zone by intermittent breaking of groups of incident

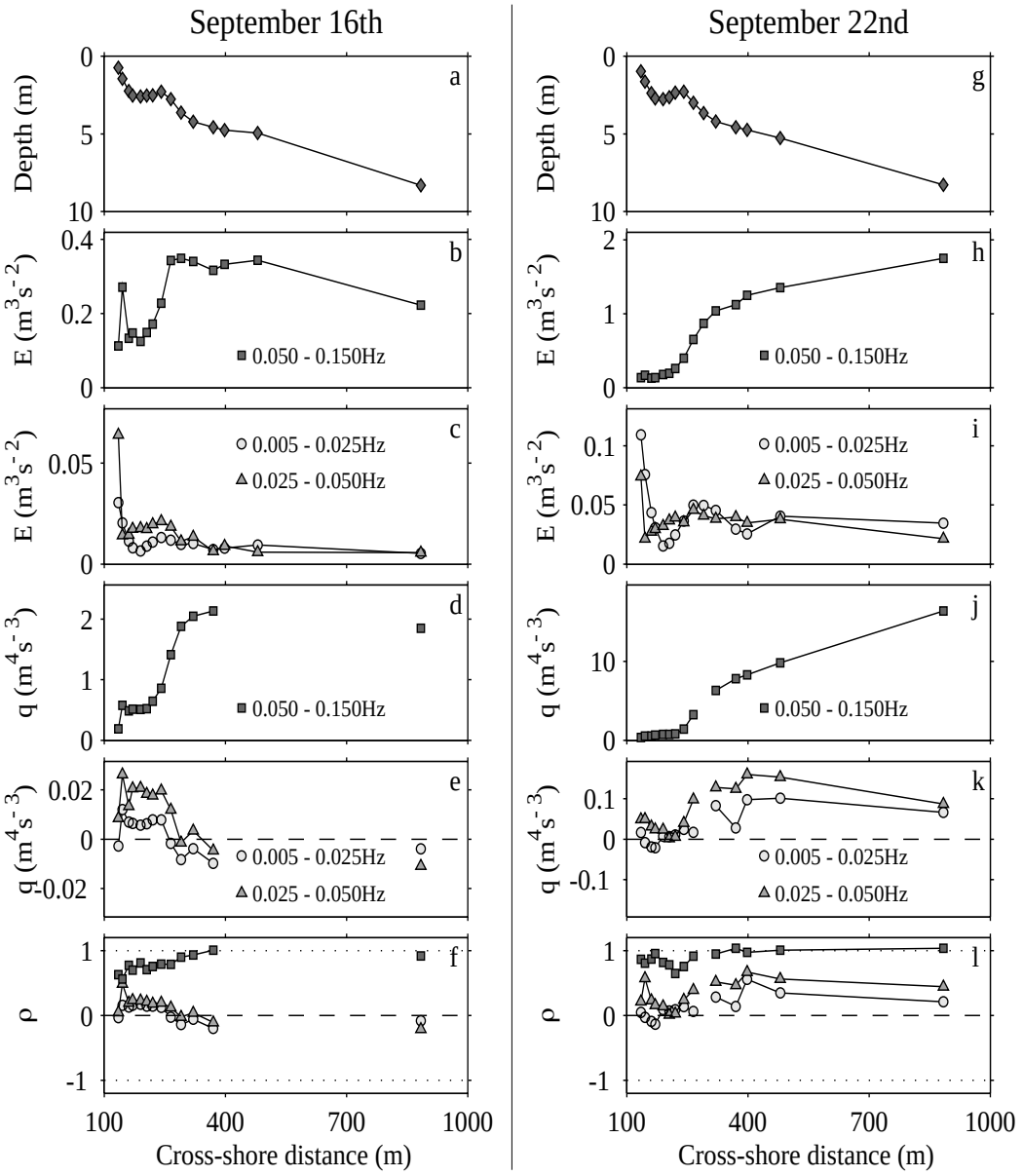

Figure 4: Water depth (a,g), swell energy density E (b,h), surf beat energy density E (c,i), swell energy flux q (d,j), surf beat energy flux q (e,k), and progressiveness parameter ρ (f,l) *versus* cross-shore distance. Values estimated from 3 hr time series. Left panels: September 16th, $Hs = 0.8$ m. Right panels: September 22nd, $Hs = 2.7$ m. Squares: Swell (0.05–0.15 Hz). Triangles: High frequency surf beat (0.025–0.05 Hz). Circles: Low frequency surf beat (0.005–0.025 Hz).

waves. Longuet-Higgins and Stewart (1962), and others suggested that surf beat is forced by groups of non-breaking waves, and that this forcing is most effective just outside the surf zone (see also Herbers *et al.* (1995)). The observed concentration of surf beat forcing at the outer edge of the surf zone is consistent with both of these theories.

The shoreward surf beat energy flux decreased close to the shore (< 1 m water depth, fig. 4e). The mechanism responsible for dissipating the surf beat energy brought into this region is not known. Bottom friction, wave breaking, and nonlinear wave interactions probably play a role, but the relative importance of these processes cannot be determined from these measurements.

For these moderately energetic waves, the ρ values for surf beat were close to zero (indicating a fairly strong cross-shore standing structure), although ρ was slightly more positive for relatively high frequency surf beat (fig. 4f).

The energy density and energy flux of energetic swell (Sept. 22nd, $Hs = 2.7$ m) decreased across the entire array (fig. 4h,j), suggesting that the surf zone extended from the shore to about 8-m water depth. The ρ values for swell were close to 1 (fig. 4l), although they dropped slightly below 1 over the bar (perhaps due to an increased directional spread of swell on the bar crest (Herbers *et al.* (1999))).

The surf beat energy flux was directed shorewards ($q > 0$, fig. 4k) across almost the entire array, indicating that the nearshore was a net sink of surf beat energy. The shoreward flux of surf beat energy decreased markedly on the offshore face of the bar (between $x \approx 200$ and $x \approx 400$ m), suggesting that surf beat was dissipated there.

Surf beat ρ values often were greater than zero and sometimes exceeded 0.5 (fig. 4l), indicating shoreward progressiveness. The ρ values of relatively high frequency surf beat were greater than ρ values of low frequency surf beat, indicating that high frequency surf beat was more shoreward-progressive than low frequency surf beat.

5 Summary

Frequency-domain EOF's based on observations of near-bottom pressure and velocity along a cross-shore transect between the shore and 8-m water depth on a barred beach were used to identify the dominant spatially coherent components of surf beat. The dominant EOF's at relatively low beat frequencies (0.005–0.025 Hz) were consistent with standing wave theories. In contrast, the dominant EOF's at relatively high beat frequencies (0.03–0.05 Hz) displayed a mixture of progressive and standing wave behaviours. The net shoreward energy flux carried by propagating surf beat, estimated from the co-spectrum between pressure and velocity fluctuations, was sometimes as large as half the energy flux that could have been carried if all surf beat propagated directly shorewards, consistent with partially progressive waves.

Surf beat carried energy towards the shore, where it was lost in water less than 1 m deep. The cross-shore surf beat energy flux also converged on the seaward side of the bar during a storm, suggesting strong surf beat dissipation there. The mechanism responsible for dissipating surf beat is not known, but bottom friction, wave breaking,

and nonlinear wave interactions might play a role.

On one occasion surf beat carried energy seawards just outside the surf zone and shorewards just inside the surf zone. The resulting net flux of surf beat energy away from the outer edge of the surf zone indicates that surf beat was forced at the outer edge of the surf zone.

Acknowledgments This research was supported by the Izaak Walton Killam Foundation, the Natural Sciences and Engineering Research Council of Canada, and the US Office of Naval Research. R.T. Guza was a principal investigator in the field program (Duck94), and contributed to all aspects of the field observations presented here. E.L. Gallagher, B. Raubenheimer, and T.H.C Herbers also made valuable contributions to the field program. Excellent logistical support was provided by staff of the Center for Coastal Studies at the Scripps Institution of Oceanography and the Field Research Facility of the U.S. Army Engineer Waterways Experiment Station's Coastal Engineering Research Center.

References

Elgar, S., Herbers, T., and Guza, R., 1994: Reflection of ocean surface gravity waves from a natural beach. *Journal of Physical Oceanography*, **24**, 1503–1511.

Elgar, S., Guza, R., Raubenheimer, B., Herbers, T., and Gallagher, E. L., 1997: Spectral evolution of shoaling and breaking waves on a barred beach. *Journal of Geophysical Research*, **102**, 15797–15805.

Gallagher, E. L., Elgar, S., and Guza, R., 1998: Observations of sand bar evolution on a natural beach. *Journal of Geophysical Research*, **103**, 3203–3215.

Gallagher, E., Boyd, W., Elgar, S., Guza, R., and Woodward, B., 1996: Performance of a sonar altimeter in the nearshore. *Marine Geology*, **133**, 241–248.

Herbers, T., Elgar, S., and Guza, R., 1995: Generation and propagation of infragravity waves. *Journal of Geophysical Research*, **100**, 24863–24872.

Herbers, T., Elgar, S., and Guza, R., 1999: Directional spreading of waves in the nearshore. *Journal of Geophysical Research*, **104**, 7683–7693.

Holland, K., Raubenheimer, B., Guza, R., and Holman, R., 1995: Runup kinematics on a natural beach. *Journal of Geophysical Research*, **100**, 4985–4993.

Holman, R., 1981: Infragravity energy in the surf zone. *Journal of Geophysical Research*, **86**, 6442–6450.

Lee, G. and Birkemeier, W., 1993: . Beach and nearshore survey data: 1985–1991, CERC field research facility. In *Technical Report CERC-93-3*. U.S. Army Corps of Engineers, Waterways Exp. Stn, Vicksburg, Miss.

Lippmann, T., Herbers, T., and Thornton, E., 1999: Gravity and shear wave contributions to nearshore infragravity wave motions. *Journal of Physical Oceanography*, **29**, 231–239.

Longuet-Higgins, M. and Stewart, R., 1962: Radiation stress and mass transport in gravity waves, with application to 'surf beats'. *Journal of Fluid Mechanics*, **13**, 481–504.

Symonds, G., Huntley, D., and Bowen, A., 1982: Two-dimensional surf beat: Long wave generation by a time-varying breakpoint. *Journal of Geophysical Research*, **87**, 492–498.